NRC Research Press

ARTICLE

Forensic application of DNA barcoding for identification of illegally traded African pangolin scales

Monica Mwale, Desire L. Dalton, Raymond Jansen, Marli De Bruyn, Darren Pietersen, Prudent S. Mokgokong, and Antoinette Kotzé

Abstract: The escalating growth in illegal wildlife trade and anthropogenic habitat changes threaten the survival of pangolin species worldwide. All eight extant species have experienced drastic population size reductions globally with a high extinction risk in Asia. Consequently, forensic services have become critical for law enforcement, with a need for standardised and validated genetic methods for reliable identifications. The seizure of three tonnes of pangolin scales, believed to have originated from Africa, by Hong Kong Customs Authorities provided an opportunity for the application of DNA barcoding in identifying scales. Three mitochondrial DNA gene regions (COI, Cyt *b*, and D-loop) were amplified for a subsample of the confiscated material and compared with taxonomically verified references. All four African species were recovered as monophyletic with high interspecific uncorrected p-distance estimates (0.048–0.188) among genes. However, only three of four African species (*Phataginus tricuspis*, *Phataginus tetradactyla*, and *Smutsia gigantea*, originating from West and Central Africa) and one of four Asian species (*Manis javanica* from Southeast Asia) were identified among scales. Although the assignment of unknown scales to specific species was reliable, additional genetic tools and representative reference material are required to determine geographic origins of confiscated pangolin specimens.

Key words: illegal wildlife trade, DNA barcoding, forensic genetics, pangolins, pangolin scale confiscation, *Smutsia*, *Manis*.

Résumé : La croissance constante du commerce illégal d'espèces sauvages et les changements d'habitat d'origine anthropogénique menacent la survie d'espèces de pangolin à l'échelle mondiale. Les huit espèces existantes ont connu des réductions dramatiques de taille de leurs populations globalement et sont à fort risque d'extinction en Asie. Conséquemment, des services de criminalistique sont devenus critiques pour assurer le respect des lois. Similairement, une standardisation et une validation des méthodes génétiques pour l'identification fiable des espèces sont nécessaires. La saisie par les autorités douanières de Hong Kong de trois tonnes d'écailles de pangolins, soupçonnées provenir d'Afrique, ont fourni l'opportunité de faire appel aux méthodes de codage à barres de l'ADN pour l'identification des écailles. Trois régions de l'ADN mitochondrial (COI, Cyt *b* et la boucle D) ont été amplifiées au sein d'un échantillon du matériel confisqué et les séquences ont été comparées à des références taxonomiques vérifiées. Les quatre espèces africaines ont été trouvées et formaient un clade monophylétique avec de grandes distances p non corrigées (0,048-0,188) parmi ces gènes. Cependant, seules trois des quatre espèces africaines (*Phataginus tricuspis*, *Phataginus tetradactyla* et *Smutsia gigantea*) provenant de l'Afrique centrale et de l'ouest ainsi qu'une des quatre espèces asiatiques (*Manis javanica*) provenant du Sud-Est de l'Asie ont été identifiées au sein des écailles. Bien que la correspondance entre les écailles d'origine inconnue et des espèces spécifiques se soit avérée fiable, des outils génétiques et des matériels de référence représentatifs additionnels sont nécessaires afin de déterminer l'origine géographique du matériel confisqué. [Traduit par la Rédaction]

Mots-clés : commerce illégal d'espèces sauvages, codage à barres de l'ADN, génétique criminalistique, pangolins, confiscation d'écailles de pangolin, *Smutsia*, *Manis*.

Received 18 July 2016. Accepted 31 August 2017.

Corresponding Editor: Dirk Steinke.

M. Mwale and P.S. Mokgokong. National Zoological Gardens of South Africa (NZG), P.O. Box 754, Pretoria 0001, South Africa.
D.L. Dalton and M. De Bruyn. National Zoological Gardens of South Africa (NZG), P.O. Box 754, Pretoria 0001, South Africa; Genetics Department, University of the Free State (UFS), P.O. Box 339, Bloemfontein 9300, South Africa.
R. Jansen. Department of Environmental, Water and Earth Sciences, Tshwane University of Technology (TUT), P/Bag X680, Pretoria 0001, South Africa; African Pangolin Working Group (APWG).
D. Pietersen. African Pangolin Working Group (APWG).
A. Kotzé. National Zoological Gardens of South Africa (NZG), P.O. Box 754, Pretoria 0001, South Africa; Genetics Department, University of the Free State (UFS), P.O. Box 339, Bloemfontein 9300, South Africa; African Pangolin Working Group (APWG).
Corresponding author: Monica Mwale (email: monicam@nzg.ac.za).

Introduction

The illegal poaching and trade of wildlife is a major biodiversity challenge that has contributed to a significant decline in populations of several species in Africa (Challender et al. 2015*b*). An increase in illegal wildlife trade has been documented for all species of pangolins (family Manidae) that are exploited for bush meat as well as body parts and scales, which have superstitious value and use in traditional medicine in Africa (*muthi*) and East Asia (Newton et al. 2008; Boakye et al. 2015; Zhang et al. 2015; Nijman et al. 2016). The illegal wildlife trade has been estimated to be worth US$2.5 billion a year in East Asia and the Pacific, with pangolins contributing an estimated US$100–150 million in Asia-Pacific (Zhang et al. 2015; Nijman et al. 2016). Therefore, illegal pangolin trade has continued to escalate, with pangolins now being the most trafficked wild mammal species by numbers (>10 000 individuals per year) globally (Davis 2014; Challender et al. 2015*a*). Furthermore, anthropogenic threats such as agricultural intensification have resulted in pangolin declines due to habitat loss and fragmentation (IUCN 2015). Particularly in South Africa, pangolins are electrocuted by electric fencing used on game and livestock farms (Bräutigam et al. 1994; Pietersen et al. 2014*a*). Pangolins are also considered to be highly vulnerable to extinction owing to their slow growth rates and low reproductive and recovery rates in impacted areas (Pietersen et al. 2014*a*). There is also very limited information available on the abundance and distribution of all species, which are all regarded as data deficient (IUCN 2015; Boakye et al. 2016).

Eight extant species are recognised (Gaudin et al. 2009), with four species distributed (Fig. 1) in the Afrotropics (giant ground pangolin, *Smutsia gigantea*; Temminck's ground pangolin, *S. temminckii*; black-bellied pangolin, *Phataginus tetradactyla*; and white-bellied pangolin, *P. tricuspis*) and four species in the Indomalayan regions of Asia (Indian pangolin, *Manis crassicaudata*; Philippine pangolin, *M. culionensis*; Sunda pangolin, *M. javanica*; and Chinese pangolin, *M. pentadactyla*). All species are considered to be threatened according to the International Union for Conservation of Nature Red List (IUCN 2015), with the four African species listed as vulnerable (Pietersen et al. 2014*b*; Waterman et al. 2014*a*, 2014*b*, 2014*c*) and the Asian species listed as endangered (two species) (Baillie et al. 2014; Lagrada et al. 2014) or critically endangered (two species) (Challender et al. 2014*a*, 2014*b*). All species were up-listed from Appendix II to Appendix I of the Convention on International Trade in Endangered Species of Wild Fauna and Flora (CITES) at the 17th meeting of the Conference of the Parties, which bans all international trade and provides for better domestic protection in Asia (Dixon and Weiskotten 2016). Therefore, effective enforcement of the existing legislation to address this unsustainable global criminal enterprise is needed. Reliable and accurate species identification is crucial for forensic investigation of cases where only processed animal parts are confiscated to assist with the monitoring and legal protection of pangolins.

Studies that have applied DNA technologies for forensic wildlife species identification have shown that species and even populations can be distinguished with mitochondrial DNA (mtDNA) genes such as cytochrome c oxidase 1 (COI), cytochrome *b* (Cyt *b*), and the control region (D-loop) (Hsieh et al. 2001; Branicki et al. 2003; Ogden and Linacre 2015). For example, the COI gene, which is considered the standard DNA barcoding region for species identification (Hebert et al. 2003), has shown high levels of distinction among wildlife species (Dawnay et al. 2007; Mwale et al. 2015). While applications of DNA technologies in forensic crime investigation have been conducted for pangolin bush meat and scales (Hsieh et al. 2011; Gaubert et al. 2015; Zhang et al. 2015), these have mainly had a limited species representation or an Asian focus or have analyzed only a single mtDNA gene. Furthermore, some published GenBank (National Center for Biotechnology Information) sequence data for pangolin species are incorrect and are based on taxonomically misidentified specimens, making species assignments unreliable (Hassanin et al. 2015; Gaubert and Antunes 2015). Reference data for different gene markers that would enable reliable forensic identification of all African pangolin species are still lacking at present for legal enforcement of wildlife crimes involving pangolin poaching and seizures.

In this study we report on forensic species identification of pangolin scales seized in Hong Kong using the COI barcoding gene and Cyt *b* and D-loop gene regions. Our analysis includes (*i*) verification of the mtDNA test using Barcode of Wildlife Project DNA barcoding reference samples to distinguish between pangolin species, (*ii*) identification of species and the origin of confiscated samples, and (*iii*) analysis of species composition of the confiscated samples.

Materials and methods

Sampling and DNA extraction

Reference tissue voucher specimens (n = 15) of three African pangolin species, viz. *S. temminckii*, *P. tetradactyla*, and *P. tricuspis*, were obtained from the National Zoological Gardens of South Africa (NZG) (see www.barcodewildlife.org) species reference database (Mwale et al. 2015) (Table 1). All voucher specimens were identified by a taxonomic expert (Ray Jansen, African Pangolin Working Group). Tissue samples of *P. tetradactyla* and *P. tricuspis* were collected in West Africa (Fig. 2A) (Boakye et al. 2016), while *S. temminckii* samples were mainly collected in South Africa (Du Toit et al. 2014) (Table 1). In addition, reference samples were supplemented with sequences of *S. gigantea* and two Asian pangolin species (*M. javanica* and *M. pentadactyla*) retrieved from GenBank (Qin et al. 2012; Hassanin et al. 2015) and the Barcode of Life Data Systems version 4 (beta) for the COI gene (Ratnasingham and Hebert 2007). These

Fig. 1. Global distribution of pangolin species according to the IUCN Red Data List of species (IUCN 2015). The sampling sites where the reference material for three African pangolin species was collected (⊙) are also indicated. Inset map is for the Philippine pangolin distribution.

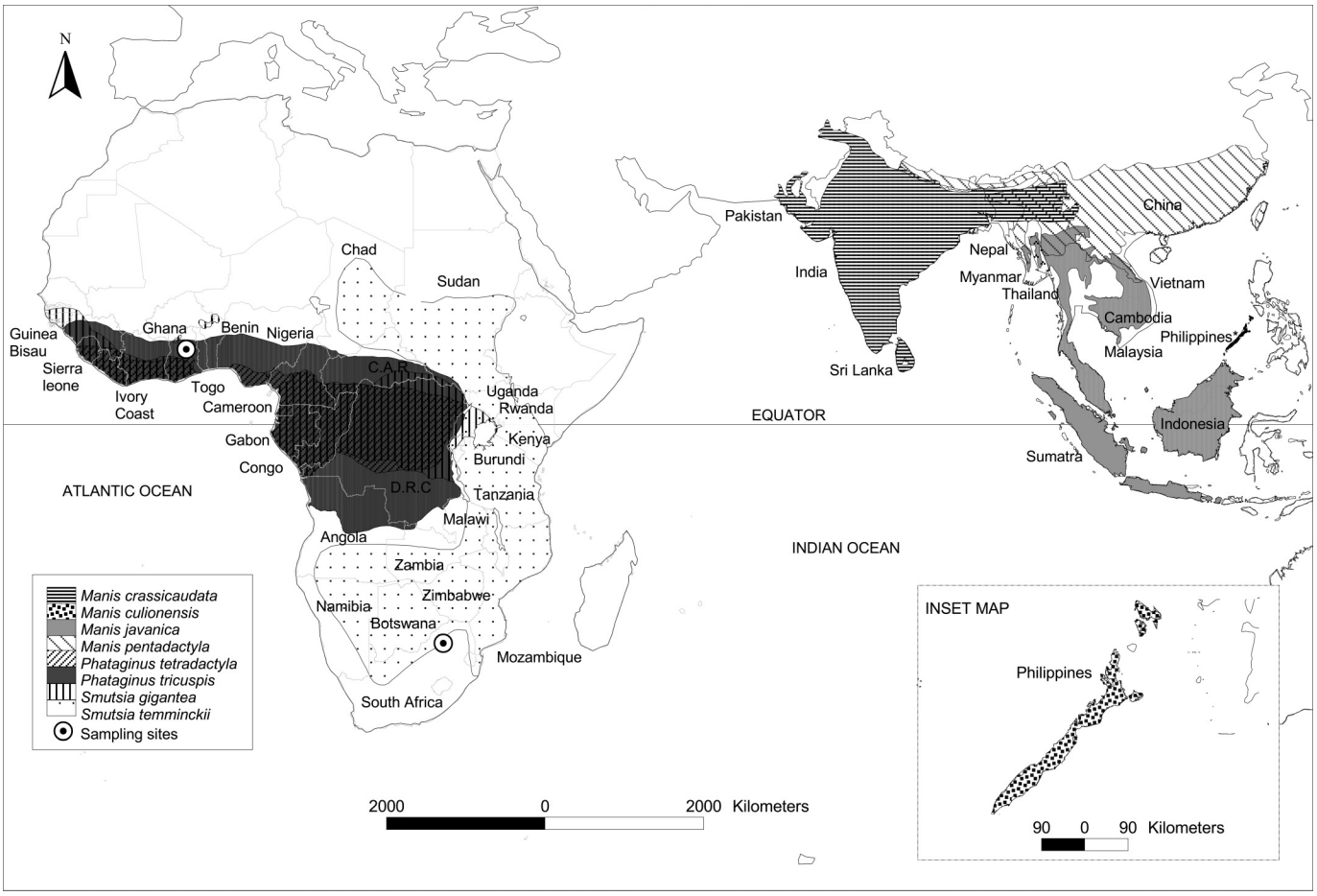

sequences were carefully selected to exclude samples where species misidentifications have been reported in recent publications (Hassanin et al. 2015; Gaubert and Antunes 2015). Suitable DNA sequences were available for six of the eight recognised pangolin taxa (Table 1) for testing of species boundaries and identification of the unknown scales.

The unidentified pangolin scales are a subset of 3.3 tonnes of scales that were illegally traded and were confiscated by the CITES Management Authority in Hong Kong between 2014 and 2015, and are thought to have originated from Africa. A representative subsample of these confiscated scales consisting of 10 bags, each representing a different consignment with a scale net weight of 27.822 kg, was exported to the NZG for analysis. Each of the bags was accessioned and assigned a unique NZG Biobank accession number. The contents of each bag (Fig. 2B) were visually sorted into distinct scale types and were assigned to a species by the taxonomic expert based on their shape, colouration, and morphology. A maximum of five samples per scale morph type (putative species) were selected from each of the 10 bags for molecular characterisation.

Scale samples were pulverised using an electric dental micro-motor drill (Zhengzhou Xinghua Dental Equipment, Henan, China). DNA was extracted using the QIAamp® DNA Investigator Kit (Qiagen Inc., Valencia, Calif., USA) following the manufacturer's instructions for degraded samples. DNA quantification for purity, concentration, and yield was performed using a NanoDrop ND-1000 spectrophotometer (Thermo Scientific, Lithuania). Extracted DNA was stored at –20 °C.

PCR amplification and sequencing

Polymerase chain reaction (PCR) was performed in 25 μL reactions that consisted of 5–20 ng of template DNA, 12.5 μL of 2× DreamTaq PCR Mastermix (Life Technologies), 10 pmol of each primer (Table 2), and double-distilled water. The thermal cycling was done according to published sources and optimisations as indicated in Table 2 (Kocher et al. 1989; Folmer et al. 1994). PCR products were visualised on 2% agarose gel before being purified using the ExoSAP protocol (Thermo Scientific, Lithuania). Purified PCR products were cycle sequenced using the BigDye Terminator v3.1 Cycle Sequencing Kit (Applied Biosystems, Foster City, Calif., USA) and then

Table 1. GenBank accession numbers and sampling localities of DNA sequence data that were used in the species reference data set and as out-groups.

Species	Locality	COI	Cyt *b*	D-loop
Smutsia gigantea	Cameroon*	KJ192837, KJ192838	KJ193382	Unavailable
Smutsia temminckii	Tanzania†	**KP306515**	**KP306515**	**KP306515**
	South Africa (NZG reference)	KX012661	Submitted	Submitted
Phataginus tetradactyla	Cameroon*	KJ192841, KJ192842	Unavailable	Unavailable
	Ghana (NZG reference)	KX012676, KX012678, KX0126779, KX012684	Submitted	Submitted
Phataginus tricuspis	Gabon†	**KP306514**	**KP306514**	**KP306514**
	Cameroon, Ghana, Nigeria*	KJ192992, KJ192849	KJ193401, KJ193402, KJ193526	Unavailable
	Ghana (NZG reference)	KX012680–KX012685	Submitted	Submitted
Manis javanica	Thailand†	**KP306516**	**KP306516**	**KP306516**
	Malaysia‡	KF007331	Unavailable	Unavailable
Manis pentadactyla	China§	KC690306, KC690307	Unavailable	Unavailable
	Thailand¶	Unavailable	KP261032 KP261034	Unavailable
Canis latrans	USA, Nebraska‡	NC_008093	NC_008093	NC_008093
Ceratotherium simum	—	NC_001808	NC_001808	NC_001808
Rhinolophus monoceros	—	NC_005433	NC_005433	NC_005433

Note: Reference pangolin species sequences (bold font) are published and verified genome or gene sequences of each species. Reference sequences were sourced from the NZG reference database.

*Gaubert et al. (2015).
†Hassanin et al. (2015).
‡GenBank sequence.
§Qin et al. (2012).
¶Gaubert and Antunes (2015).

Fig. 2. Pangolins from the bush meat trade in West Africa (A) and scales from the Hong Kong confiscation (B).

purified with a ZR DNA Sequencing Clean-up Kit (Zymo Research Corporation, Irvine, Calif., USA). Sequencing products were visualised with an ABI 3500 genetic analyser (Applied Biosystems, Foster City, Calif., USA).

Sequence assembly and phylogenetic analyses

Consensus sequences for each mtDNA gene were edited and assembled separately and then aligned using MUSCLE (Edgar 2004) in Geneious v8.1.6 (Biomatters Ltd., Auckland, New Zealand). All mtDNA haplotypes were deposited in GenBank (Table 1). The best-fit model of nucleotide substitution for each data set was estimated using the Bayesian Information Criterion implemented in jModelTest 2.1.7 under default parameters (Guindon and Gascuel 2003; Darriba et al. 2012). Neighbour-joining (NJ) analyses were conducted using the selected models of evolution (with invariable sites) in Geneious for all the gene and concatenated data sets. The topology of the NJ tree was confirmed with Bayesian Markov Chain Monte Carlo analyses (BI) as implemented in MrBayes 3 (Ronquist et al. 2012) in Geneious. Default settings were used and simulations were run for 1 100 000 generations (burn-in = 100 000) until the standard deviation of split frequencies was below 0.01.

Species delimitation in pangolins and forensic identification

Species distinction was evaluated using the Basic Local Alignment Search Tool (BLAST) of the NCBI database in Geneious and phylogenetic analyses of sequence characters. The NCBI BLAST (Altschul et al. 1990) uses an alignment program to determine the identity of unknown organisms based on pairwise DNA nucleotide comparisons (percentage matches) of gene sequences accessioned by researchers into this database. The phylogenetic analyses used two different approaches: (1) species tree analyses using each gene and annotated genome sequences and (2) analysis of a concatenated data set of all three gene fragments. The concatenated data set was tested for congruence using the Incongruence Length Difference (ILD) Test in PAUP* v4.0b10 (Swofford 2002), where critical

Table 2. PCR conditions and primer sequences used for sequencing three pangolin mitochondrial DNA gene fragments.

Gene	PCR cycling conditions	Primers	Source	Fragment length (bp)	BIC best-fit model	Variable sites (PS)	Informative sites (PI)
COI	40 cycles: 30 s at 94 °C, 40 s at 45 °C (×5) | 51 °C (×35), 90 s at 72 °C	dgLCO1490, dgHCO2198; Pan6AF, PAN6AR	Folmer et al. 1994; Du Toit et al. 2014	600	HKY+I (I = 0.631)	200 (33.0%)	147 (24.5%)
Cyt *b*	15 cycles: 30 s at 94 °C, 50 s at 60 °C (×5) | 55 °C (×10), 60 s at 72 °C	Cytb_Univ1, Cytb_Univ2	Kocher et al. 1989	400	HKY+I (I = 0.631)	133 (33.2%)	109 (27.2%)
D-loop	30 cycles: 30 s at 94 °C, 30 s at 50 °C, 45 s at 72 °C	Pan_15A_F, Pan_15A_R	Hsieh et al. 2011	576	HKY+G (G = 0.267)	131 (22.7%)	114 (19.8%)
All genes	—	—	—	1576	HKY+G (G = 0.170)	430 (27.3%)	217 (13.8%)

Note: Sequence information for the different gene fragments is also provided. BIC, Bayesian Information Criterion.

values for the test are between 0.01 and 0.001 (Farris et al. 1994; Cunningham 1997). Published mtDNA genome gene sequences (Table 1) from the three closely related orders suggested by Hassanin et al. (2015) were used to root the trees.

Species boundaries were verified from the phylogenetic trees using the Species Delimitation Plugin (SDP) in Geneious (Masters et al. 2011) and a standard barcoding gap analysis for the COI data based on Kimura 2-parameter (K2P) distances using the Automatic Barcode Gap Discovery (ABGD) method (Puillandre et al. 2012) with default parameters. The SDP delimits species by evaluating the phylogenetic exclusivity or monophyly of clades by testing the probability of this monophyly occurring by chance in a coalescent process (Masters et al. 2011). SDP also assesses the probability with which a putative species can be diagnosed successfully on a phylogenetic tree by comparing intra- and interspecific genetic distances among well-supported monophyletic clades (bootstrap ≥70%).

The ABGD method uses several prior thresholds for the partitioning of sequences into primary species based on the "barcode gap", which compares the distribution of pairwise differences between intraspecific and interspecific diversity among different species (Hebert et al. 2003) without an a priori species hypothesis. The ABGD analysis estimates the relative gap width and the minimum and maximum values of prior intraspecific divergence, which are used to detect the barcode gap using the default K2P model. Default settings of prior minimum genetic distances range from 0.001 to 0.1 on the ABGD website (http://wwwabi.snv.jussieu.fr/public/abgd), as these default *P* values typically produce a range of operational taxonomic unit (OTU) counts (Puillandre et al. 2012). In both delimitation methods, a species is distinct from its nearest neighbour (NN) if its maximum intraspecific distance is less than the distance to its NN sequence. Barcode gaps between well-supported clades of haplotypes identified by NJ and BI were taken as an indication of separate molecular operational taxonomic units (MOTUs). Therefore, barcode gaps and sequence divergences between well-supported clades identified by phylogenetic analyses were taken as an indication of separate species or OTUs.

Results

Species reference data set and DNA barcoding analyses

Sequence alignment yielded sequence fragments of 600, 400, and 576 base pairs for COI, Cyt *b*, and D-loop, respectively (Table 2). The HKY85 model (Hasegawa et al. 1985) was selected as the best-fit model of evolution for all gene fragments using jModelTest. The topologies of the NJ and BI gene trees and concatenated mtDNA data set (Fig. 3) were similar with regards to species relationships and clusters. All six reference species (*P. tricuspis*, *P. tetradactyla*, *S. gigantea*, *S. temminckii*, *M. javanica*, and

Fig. 3. Inter- and intraspecific relationships among African (black bars) and Asian (grey bars) pangolin species used as reference material for the Cyt *b* (A) and COI (B) data sets. Values on the branches are bootstrap support values (below) and posterior probabilities (above; only posterior probabilities >0.95 are indicated) for all the phylogenetic analyses. The D-loop data set received 100% bootstrap and 1.00 posterior probability support for all clades and all species and values are therefore not indicated. Black nodes indicate substructuring in *Phataginus tricuspis*.

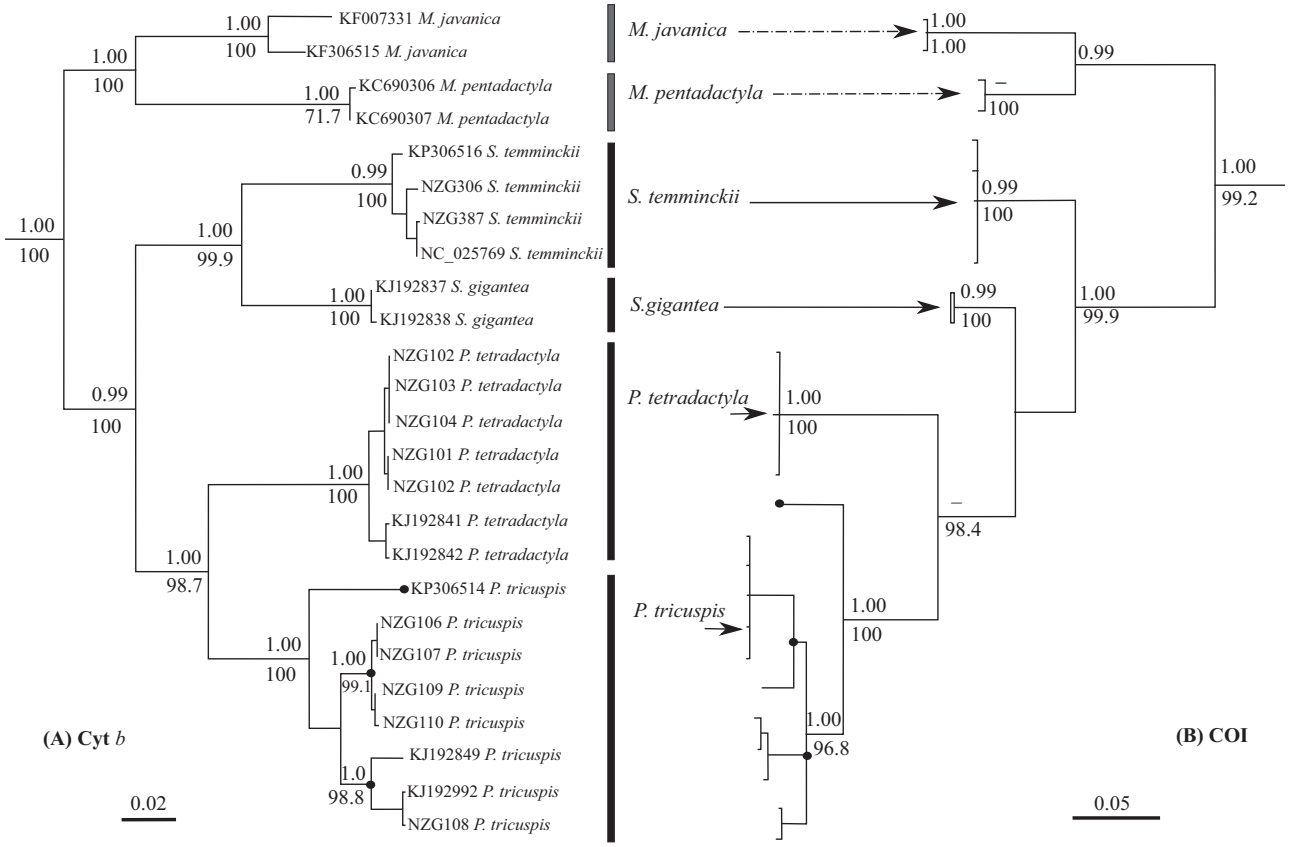

M. pentadactyla) were recovered and well supported with high (>70%) bootstrap support. Interspecific p-distance estimates between all species clades were high: 0.100–0.188 for COI and 0.10–0.20 for Cyt *b* (Tables 3 and 4), and 0.048–0.125 for D-loop. African specimens were also recovered as monophyletic (96%–100% bootstrap support: all genes), sharing a most recent common ancestor (MRCA) that was distinct from the Asian pangolin lineage (*Manis* spp.). All four African pangolin species were further recovered as NN taxa or sister taxa within the two African genera (Fig. 3). The concatenated reference data set (supplementary data, Fig. S1[1]) of all genes (ILD tested) produced a fully resolved tree with strong bootstrap (>91%) and posterior probability (>0.99) support for monophyletic distinction among all species and genera, indicating that a combined gene analysis provides better phylogenetic signal.

The results of the SDP analyses for COI, Cyt *b*, and D-loop using the phylogenetic trees (BI) were similar and are summarised in Table 4. The SDP analyses of all genes provided support for the distinction of all six species, yielding high values for the two *P* (ID) estimates and their mean probabilities at 95% confidence intervals (Table 4). These results indicated that the species reference samples were significantly different ($P < 0.05$) from each other and represented distinct species under the same coalescent model of evolution. The mean intraspecific p-distances ranged from 0.001 to 0.055 (all mtDNA genes) among all species with *M. javanica* and *P. tricuspis* (COI data: 0.037 and 0.030, respectively), having higher maximum intraspecific divergences, suggesting geographic substructuring. The observed trend of higher sequence divergence was also reflected in the Cyt *b* (Table 4) and D-loop (not indicated) analyses for *P. tricuspis*. The ABGD analyses were robust when comparing specimens of the same species and revealed six genetic groups (MOTUs) that corresponded with the six putative species (Fig. 4) that had COI divergences ranging from 3.59%–5.99% (Fig. 4). The mean overall interspecific p-distance was high (20.0%–22.8%) and significantly different ($P < 0.05$) between the three genera, providing support for delimitation at the genus level within Manidae.

[1]Supplementary data are available with the article through the journal Web site at http://nrcresearchpress.com/doi/suppl/10.1139/gen-2016-0144.

Table 3. Interspecific sequence divergence estimates (mean ± standard error) for the COI (above diagonal) and Cyt *b* (below diagonal) gene regions of the species reference data set.

Species	*S. gigantea*	*S. temminckii*	*P. tetradactyla*	*P. tricuspis*	*M. javanica*	*M. pentadactyla*
Smutsia gigantea		0.115±0.013	0.183±0.016	0.160±0.016	0.150±0.014	0.180±0.016
Smutsia temminckii	0.103±0.017		0.185±0.016	0.188±0.016	0.182±0.015	0.177±0.015
Phataginus tetradactyla	0.134±0.018	0.161±0.019		0.150±0.014	0.149±0.014	0.100±0.012
Phataginus tricuspis	0.144±0.019	0.145±0.019	0.151±0.019		0.102±0.012	0.165±0.015
Manis javanica	0.162±0.016	0.160±0.016	0.174±0.016	0.106±0.011		0.145±0.013
Manis pentadactyla	0.199±0.022	0.196±0.022	0.200±0.021	0.179±0.021	0.154±0.016	

Identification of unknown scales: species assignment tests

DNA from 53 confiscated scales was extracted for species identification. The BLAST searches of all three genes indicated that the scale sequences all had 88%–100% pairwise identity with six pangolin species (*P. tricuspis*, *P. tetradactyla*, *S. gigantea*, *S. temminckii*, *M. javanica*, and *M. pentadactyla*) and unidentified Asian records (*Manis* sp.; 100% match; Table 5). However, examination of the low pairwise matches (88%–90%) within species showed that these matches were all for comparisons with misidentified GenBank records incorrectly accessioned as *M. pentadactyla* or *P. tetradactyla*, which have been noted in recent studies (Hassanin et al. 2015; Gaubert and Antunes 2015). Although the COI match to *S. temminckii* was also low (Table 5: 89%–90%), this match was considered to be an interspecific match within *Smutsia* based on the genetic diversities in the reference data (Table 3). Exclusion of low pairwise matches (interspecific) and misidentified samples improved the BLAST matches to a minimum of 93.4% (COI), 95.3% (Cyt *b*), and 93.2% (D-loop). The lowest NCBI BLAST matches (89.0%–93.5%) were all among *Manis* and *Phataginus* species records, probably because of high intraspecific divergence (COI) and lack of reference material for the D-loop. Furthermore, the high range of variation within *P. tricuspis* (93.4%–100%), which has been noted in the literature (Hassanin et al. 2015), suggests genetic substructuring. Matching sequence identity between scale sequences and the verified reference samples (this study) further improved the accuracy (95%–100%) in matching scales to only four species, *P. tricuspis*, *P. tetradactyla*, *S. gigantea*, and *M. javanica* (Table 4). There was no accurate match between the unknown scales and either *M. pentadactyla* or *S. temminckii* (Fig. 5).

The combined SDP analyses based on reference and unknown scale phylogenetic analyses, which tested the probability that the putative species clades had the observed degree of distinctiveness, were still higher than the threshold of 0.05 (0.5–0.12). The six recovered putative species clades (including scales) had Rodrigo's *P*(Randomly Distinct) values of <0.05 (Table 4; Fig. 4), with Rosenberg's P_{AB} values being significant for all African species ($P < 0.05$), but not for the *M. javanica* species clade ($P > 0.11$), for all data sets. Rodrigo et al. (2008) defined distinctive clades as those that have *P*(Randomly Distinct) values of <0.05. High values support species distinction, while lower values may suggest cryptic speciation for branching events that would be expected under different coalescent models (Masters et al. 2011). This result may therefore support the presence of other Asian species among these scales in the "*M. javanica*" clade (Fig. 5).

The 10 pangolin bag samples were genetically identified as originating from both African and Asian pangolin species (Table 5). Six of the confiscated bags were of an African origin for three species (*S. gigantea*, *P. tetradactyla*, and *P. tricuspis*), while four were of Asian origin, representing *M. javanica* (100% node support with reference sequence) and other Asian species (*Manis* spp.) whose identity could not be verified owing to a lack of verified species reference data. Species composition analyses indicated that some of the confiscated samples represented multiple pangolin species within one bag (Table 5). One bag (NZG 46070) had multiple *Manis* species from Asia, while two of the bags contained the two African tree pangolin species (*P. tetradactyla* and *P. tricuspis*).

Discussion

The results of the phylogenetic analyses (NJ and BI) and the independent methods with a priori grouping (ABGD and SPD) that were used to investigate species diversity were generally congruent among the gene fragments and showed identical patterns with regards to species identifications. This consistent result for the reference database was critical to ensure accurate and reliable assignment of samples of unknown species. This is especially important because the current GenBank database of published pangolin sequences has limited information on African species and inaccurate information for several pangolin species (Hassanin et al. 2015; Gaubert and Antunes 2015), which can lead to poor confidence in species assignments. The observed interspecific divergence estimates of the reference database (minimum of 10% between species) were higher than the 2% that has been observed for reliable distinction among species of vertebrates for the COI and Cyt *b* regions (Hsieh et al. 2001; Hebert et al. 2003). These values were also within the range previously observed for D-loop sequences among pangolin species (Zhang et al. 2015). The level of sequence variation between individuals within *M. pentadactyla*, *M. javanica*, *S. gigantea*, and *S. temminckii*

Table 4. Summary statistics of the Species Delimitation Plugin analyses for the COI and Cyt *b* gene region data sets among six pangolin species.

Species reference	*N*	Intra distance	NN	Inter distance – NN	Intra/inter	P ID(Strict) COI	P ID(Strict) Cyt *b*	Av (MRCA-tips)	Rodrigo's *P* (Randomly Distinct)	Rosenberg's P_{AB}
1: SGI	2	0.003	2: STE	0.113 (0.113)	0.030	0.58 (0.43, 0.73)	0.59 (0.44, 0.74)	0.0001 (0)	0.05	0.03 (0.02)
2: STE	4	0.010 (0.003)	1: SGI		0.090	0.81 (0.67, 0.95)	0.91 (0.79, 1.00)	0.0081 (0.0035)	0.05	0.03 (0.02)
3: PTR	6	0.030 (0.055)	4: PTE (SGI)	0.162 (0.177)	0.190	0.91 (0.85, 0.98)	0.80 (0.69, 0.90)	0.0309 (0.0527)	0.12 (0.70)	$<10^{-4}$
4: PTE	8	0.009 (0.004)	3: PTR (SGI)	(0.168)	0.060	0.92 (0.81, 1.00)	0.92 (0.80, 1.00)	0.0081 (0.0052)	0.05	$<10^{-4}$
5: MJA	2	0.029 (0.001)	6: MPE	0.175 (0.147)	0.170	0.51 (0.36, 0.66)	0.79 (0.61, 0.96)	0.0182 (0.0008)	0.08 (0.05)	0.11 (0.02)
6: MPE	2	0.003 (0.004)	5: MJA		0.020	0.58 (0.43, 0.73)	0.77 (0.60, 0.95)	0.0011 (0.0036)	0.05 (N/A)	0.11 (0.02)
Scales ID										
1: SGI		0.006	2: STE	0.006	0.127		0.84 (0.69, 0.98)	0.0043	0.05	4.08E–03
2: STE		0.011	1: SGI	0.011	0.127		0.81 (0.67, 0.95)	0.0085	0.05	4.08E–03
3: PTR		0.032	4: PTE	0.132	0.250		0.91 (0.86, 0.97)	0.0284	0.05	9.1E–9
4: PTE		0.015	3: PTR	0.132	0.110		0.92 (0.83, 1.00)	0.0161	0.05	9.1E–9
5: MJA		0.037	6: MPE	0.154	0.240		0.47 (0.32, 0.62)	0.0184	0.05	0.11
6: MPE		0.002	5: MJA	0.154	0.010		0.58 (0.43, 0.73)	0.0010	0.05	0.11

Note: Intra/inter, ratio of intra (genetic differentiation among the members of a putative species) to inter (genetic differentiation between the members of a putative species and the members of the closest putative species); NN, nearest neighbour; P ID(Strict), mean (95% confidence interval) probability of correctly identifying an unknown member of a given clade using the criterion that it must fall within, but not sister to, the species clade in a tree; Rosenberg's P_{AB}, probability of reciprocal monophyly under a random coalescent model among taxa (the Cyt *b* values are indicated in parentheses when different from the COI estimates); scales ID, species identifications of confiscated scales that were identified during this study; SGI, *Smutsia gigantea*; STE, *S. temminckii*; PTR, *Phataginus tricuspis*; PTE, *P. tetradactyla*; MJA, *Manis javanica*; MPE, *M. pentadactyla*.

was lower than that observed in *P. tricuspis* (up to 7% BLAST mismatch), suggesting genetic substructuring in the latter species. Potential cryptic speciation has been reported in this species by Hassanin et al. (2015) , who identified a unique lineage for a Gabon sample in their genomic analyses. Although high intraspecific variation was observed, accurate identification of species was still possible because the unique lineages in *P. tricuspis* were monophyletic and shared an MRCA. Furthermore, the intraspecific pairwise differences were much lower than the interspecific values and were within the expected limit of a "barcode gap" (Puillandre et al. 2012).

The observed differences in the phylogenetic relationships among pangolin species in the COI and Cyt *b* trees for *S. gigantea* and *S. temminckii* could be attributed to a single locus analysis that can be influenced by incomplete lineage sorting (Hebert et al. 2003), as analysis of the concatenated data produced a resolved tree at all taxonomic levels. This study therefore reinforces the utility of DNA barcoding for species identification using both COI and Cyt *b* gene regions. The successful use of mtDNA markers in forensic applications for the identification of unknown animal samples to species, genus, and family levels has been demonstrated in several studies (Hsieh et al. 2001; Verma and Singh 2002; Ogden and Linacre 2015). For example, Verma and Singh (2002) demonstrated the use of Cyt *b* in the identification of 221 species of animals in forensic cases of processed unknown animal parts. The advantage of mtDNA analysis is that the technology is cost effective and simple enough for individual laboratories even with poor resources to compare sequences for thousands of species (Ratnasingham and Hebert 2007).

Furthermore, the results of this study indicate that forensic identification of all African pangolin species is reliable and effective using the COI, Cyt *b*, and D-loop mtDNA gene regions. The gene trees of the combined reference and scale sequence data set support the monophyly of all identified African groups that were in agreement with current taxonomy with very high support values (e.g., >94% for Cyt *b*). These monophyletic clades were also different from each other, with high levels of divergence providing accurate species identification (>10% COI divergence between clades). The mtDNA sequences of scales identified as being from an African origin clustered in the strongly supported monophyletic clades (90%–100% bootstrap support) of three species, viz. *S. gigantea*, *P. tetradactyla*, and *P. tricuspis*, to the exclusion of sequences from Asian pangolin species. These three African species have overlapping distributions throughout most of their range in central and western Africa (IUCN 2015). The absence of *S. temminckii* in the confiscated material and analyses may suggest that these specific African illegal trade consignments were very likely not of a southern or East African origin. *Smutsia temminckii* has the largest distribution range of the four African species and

Fig. 4. Results of the Automatic Barcode Gap Discovery analysis of the mtDNA COI gene using Kimura 2-parameter distances. This analysis was for prior intraspecific divergences for the reference data set of six putative species based on the distance at which a barcode gap occurs. OTU, operational taxonomic unit.

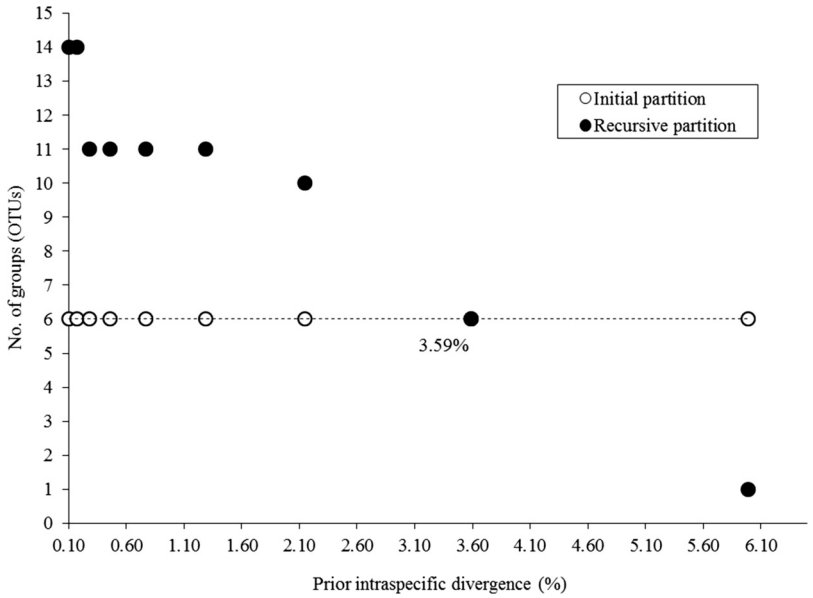

is the only pangolin species occurring in southern Africa and over most of East Africa. It is however important to note that this species' absence in the confiscated material could also indicate a reduction in the abundance of *S. temminckii* in parts of its range where it marginally co-occurs with *P. tricuspis*. *Smutsia gigantea*, a sister taxon of *S. temminckii*, has also been reported to be rare and was only identified in one bag, suggesting that species of this genus may occur at very low densities (Pietersen et al. 2014*b*) owing to previous exploitation events or anthropogenic pressure. In southern Africa, the decline in abundance has been mainly associated with habitat loss and transformation (Pietersen et al. 2014*a*), generally due to agricultural intensification and anthropogenic activities such as electrocutions (electric fencing) as well as ongoing poaching and illegal trade (traditional medicines).

This analysis also suggests that all pangolin species, including African species (*S. gigantea*, *P. tetradactyla*, and *P. tricuspis*), are targeted regionally and as a group globally with no discrimination among species on the black market. Of the 10 batches that were analysed, three were mixed-species bags (*P. tetradactyla*, *P. tricuspis*, and Asian *Manis* spp.) and seven contained a single species. The two African origin mixed-species bags contained both of the co-occurring tree pangolin species, with *P. tetradactyla* having a range that completely overlaps that of *P. tricuspis* mainly in central Africa. The analyses also indicated the presence of several Asian species in the consignment. Some scale samples were included in a strongly supported monophyletic clade with the verified *M. javanica* reference sequence and had 100% blast matches with unidentified *Manis* species. However, this clade was not supported in the SDP analysis, suggesting missing data. Reference samples are therefore required for all Asian pangolin species that either have no reference material (e.g., *M. culionensis* and *M. crassicaudata*) or lack specific accurate gene region data sets in GenBank (*M. pentadactyla*). However, the absence of a match for *M. pentadactyla*, even with verified reference Cyt *b* sequences, suggests that this trade consignment may be from a specific area in Asia and can be traced to origin with further analyses. The presence of multiple Asian species in one bag also suggests indiscriminate poaching within Asia for pangolins.

Conclusion

These findings suggest that the confiscated material could be from several sources in Africa and Asia and is therefore part of an organised illegal trade enterprise throughout the distribution range of pangolins. Knowledge of the species targeted by poachers and the areas where poaching activity may be happening is needed to develop and support effective conservation plans by authorities. However, our analyses were not able to refer the confiscated scale samples to any specific populations owing to the absence of geographically representative reference material. In addition, population-level markers such as single nucleotide polymorphisms (SNPs) would be required to accurately refer scales of unknown provenance to specific populations. Our analyses suggest that geographic identification would be possible for most pangolin species owing to the high levels of intraspecific variation that indicates substructuring in African species (*P. tricuspis*). Further analysis with geographic sampling and a SNP database for African and Asian species will facilitate a better understanding of the geographic origin of pangolin derivatives in trade, allow for better monitoring

Table 5. Species identification results from the amplified genes and top similarity matches (BLAST) of confiscated scales batches (NZG numbers) to the sequences from NCBI (in parentheses).

Bag No.	NZG Biobank No.	ID and no. of scales analysed (*n*)	COI (% BLAST match)	Cyt *b* (% BLAST match)	D-loop (% BLAST match)	Verified species ID (SDP/ABDG)
1	46066	FC288A–FC288E (5)	*P. tricuspis* (94.9)	*P. tricuspis* (99.1–99.4)	*P. tricuspis* (96.5–98)	*P. tricuspis*
2	46067	FC289A–FC289D (4)	*M. javanica* (98.2)	*M. javanica* (96.4–97.2) ***M. pentadactyla* (96.7–97)**	*Manis* sp. (91–98.5)	*M. javanica*, *Manis* sp.
3	46071	FC290A–FC290D (4)	*S. temminckii* (89–90)	*S. gigantea* (99.6–100)	Unavailable	*S. gigantea*
4	46072*	FC291A–FC291F (6) FC292A, FC292C–FC292E (4) FC292B (1)	*P. tricuspis* (95.7) ***P. tetradactyla* (88.4)**	*P. tricuspis* (98.4–100) *P. tetradactyla* (100) *P. tricuspis* (99.6)	Unavailable *P. tetradactyla* (94.0)	*P. tricuspis* *P. tetradactyla* *P. tricuspis*
5	46063*	FC293A–FC293D (4) FC294A1–FC294E1 (4)	*P. tricuspis* (94.2) *P. tetradactyla* (99.0–100)	*P. tricuspis* (99.2) *P. tetradactyla* (97.8–98.5)	*P. tricuspis* (96.7) *P. tetradactyla* (93.2–93.5)	*P. tricuspis* *P. tetradactyla*
6	46070*	FC294A2–FC294E2 (5)	*M. javanica* (99.3–100)	*Manis* sp. (100) *M. javanica* (98.7–99.1)	Unavailable	*M. javanica*, *Manis* sp.
		FC295A–FC295E (5)	Unavailable	*Manis* sp. (99.6) *M. javanica* (95.4–99.3) ***M. pentadactyla* (95.4)**	*Manis* sp. (89–89.8)	*M. javanica*, *Manis* sp.
7	46065	FC296A–FC296C (3)	*M. javanica* (100)	*M. javanica* (96.7–99.1) ***M. pentadactyla* (98)**	*Manis* sp. (97.8)	*M. javanica*, *Manis* sp.
8	46064	FC297A–FC297B (2)	Unavailable	*M. javanica* (97.2)	*Manis* sp. (89.5–93.1)	*Manis* sp.
9	46068	FC298A–FC298B (2)	*P. tricuspis* (93.7–95) ***P. tetradactyla* (95)**	*P. tricuspis* (99.1–100)	Unavailable	*P. tricuspis*
10	46069	FC299A–FC299D (4)	*P. tricuspis* (93.4–95) ***P. tetradactyla* (95)**	*P. tricuspis* (97.3–99.4) ***P. tetradactyla* (98.2)**	*P. tricuspis* (97.2)	*P. tricuspis*

Note: The species matches in bold font indicate the NCBI sequence matches of records noted as species misidentifications from publications that were within the range of closely related pangolin species. ABDG, Automatic Barcode Gap Discovery; SDP, Species Delimitation Plugin.

*Indicates bags with mixed species and scales that were sorted as different morph types before analyses.

Fig. 5. Phylogeny of the pangolin scales that were confiscated in Hong Kong in comparison with the reference species data set (bold) based on Cyt *b* mtDNA sequences. Neighbour-joining bootstrap values (below) and Bayesian inference posterior probability values (above) are indicated on the branches. Missing support values (-) indicate a lack of significant bootstrap or posterior probability support for the clade. Clades that were not identified among the confiscated scales are indicated by blue bars.

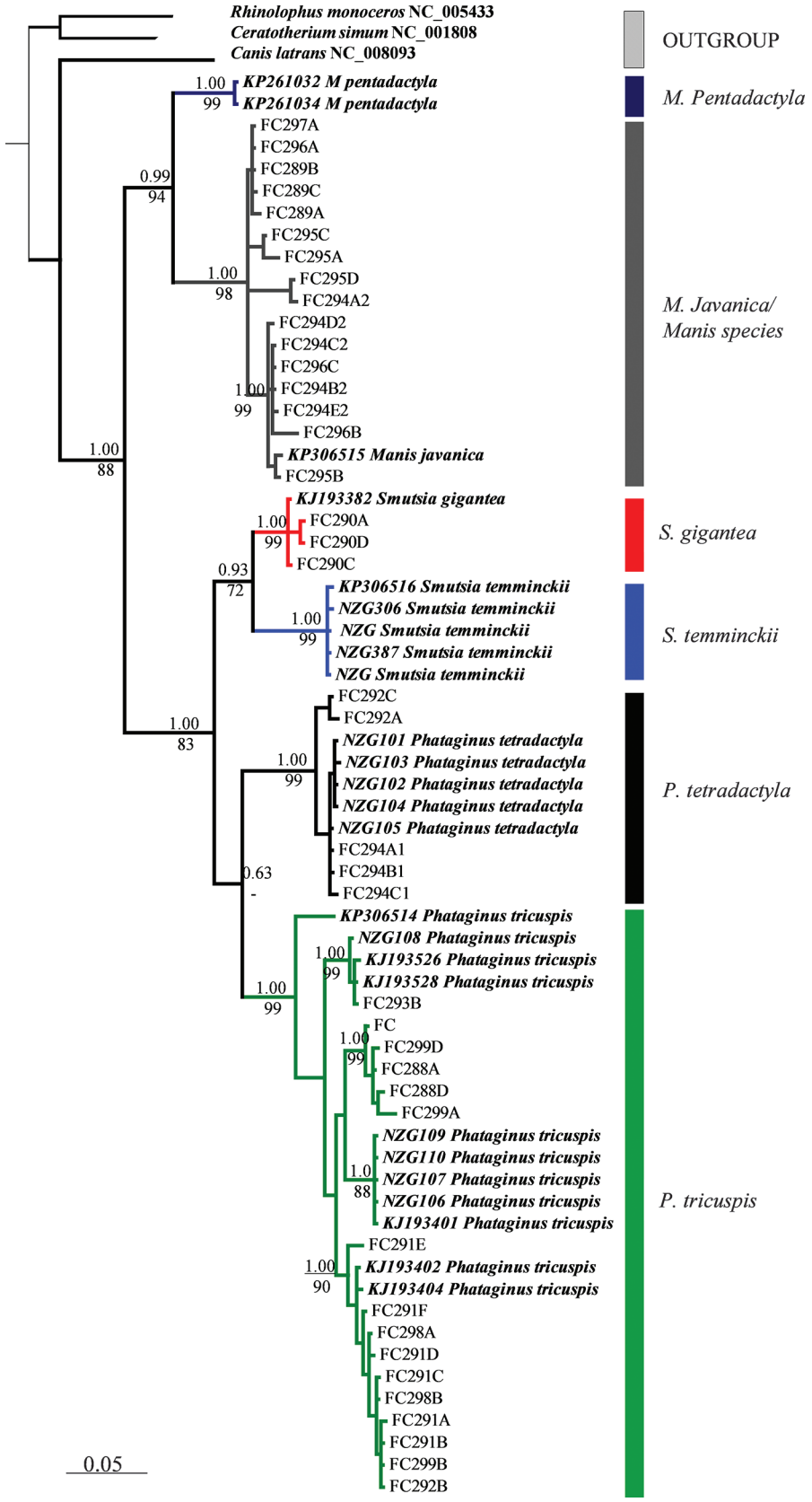

of this trade and effective law enforcement concerning illegal trade activities involving pangolins.

Acknowledgements

The authors would like to thank Maxwell Boakye (West Africa) and Amathole Museum (South Africa) for kindly providing reference material for African pangolins. Funding for DNA barcoding (COI) and the collection of chain of custody reference material was provided by the Barcode of Wildlife Project through a Google Global Impact Award to the Smithsonian Institute (David Schindel). Geographic information system files for mapping distributions were sourced from the IUCN Red Data List. The authors would like to thank Zelda Du Toit for advice on DNA extraction protocols. Kim Labuschagne, Thando Radebe, Marilise Meyer-Bouwer, Antonie Kloppers, and Takalani Musekwa are acknowledged for biobanking assistance and sampling.

References

Altschul, S.F., Gish, W., Miller, W., Myers, E.W., and Lipman, D.J. 1990. Basic local alignment search tool. J. Mol. Biol. **215**(3): 403–410. doi:10.1016/S0022-2836(05)80360-2. PMID:2231712.

Baillie, J., Challander, D., Kaspal, P., Khatiwada, A., Mohapatra, R., and Nash, H. 2014. *Manis crassicaudata*. IUCN Red List Threat. Species 2014: e.T12761A45221874.en. doi:10.2305/IUCN.UK.2014-2.RLTS.T12761A45221874.en.

Boakye, M.K., Pietersen, D.W., Kotzé, A., Dalton, D.L., and Jansen, R. 2015. Knowledge and uses of African pangolins as a source of traditional medicine in Ghana. PLoS ONE, **10**(1): e0117199. doi:10.1371/journal.pone.0117199. PMID:25602281.

Boakye, M.K., Kotzé, A., Dalton, D.L., and Jansen, R. 2016. Unravelling the pangolin bushmeat commodity chain and the extent of trade in Ghana. Hum. Ecol. **44**: 257–264. doi:10.1007/s10745-016-9813-1.

Branicki, W., Kupiec, T., and Pawlowski, R. 2003. Validation of cytochrome *b* sequence analysis as a method of species identification. J. Forensic Sci. **48**(1): 83–87. PMID:12570204.

Bräutigam, A., Howes, J., Humphreys, T., and Hutton, J. 1994. Recent information on the status and utilization of African pangolin. Traffic, **15**(1): 15–22.

Challender, D., Baillie, J., Ades, G., Kaspal, P., Chan, B., Khatiwada, A., et al. 2014*a*. *Manis pentadactyla*. IUCN Red List Threat. Species 2014: e.T12764A45222544.en. doi:10.2305/IUCN.UK.2014-2.RLTS.T12764A45222544.en.

Challender, D., Nguyen Van, T., Shepard, C., Krishnasamy, K., Wang, A., Lee, B., et al. 2014*b*. *Manis javanica*. IUCN Red List Threat. Species 2014: e.T12763A45222303.en. doi:10.2305/IUCN.UK.2014-2.RLTS.T12763A45222303.en.

Challender, D.W.S., Harrop, S.R., and MacMillan, D.C. 2015*a*. Understanding markets to conserve trade-threatened species in CITES. Biol. Conserv. **187**: 249–259. doi:10.1016/j.biocon.2015.04.015.

Challender, D.W.S., Harrop, S.R., and MacMillan, D.C. 2015*b*. Towards informed and multi-faceted wildlife trade interventions. Glob. Ecol. Conserv. **3**: 129–148. doi:10.1016/j.gecco.2014.11.010.

Cunningham, C.W. 1997. Can three incongruence tests predict when data should be combined? Mol. Biol. Evol. **14**(7): 733–740. doi:10.1093/oxfordjournals.molbev.a025813. PMID:9214746.

Darriba, D., Taboada, G.L., Doallo, R., and Posada, D. 2012. jModelTest 2: more models, new heuristics and parallel computing. Nat. Methods, **9**(8): 772. doi:10.1038/nmeth.2109. PMID:22847109.

Davis, E. 2014. 'Shocking' scale of pangolin smuggling revealed. Available from http://www.bbc.co.uk/nature/26549963 [accessed 22 January 2016].

Dawnay, N., Ogden, R., McEwing, R., Carvalho, G.R., and Thorpe, R.S. 2007. Validation of the barcoding gene COI for use in forensic genetic species identification. Forensic Sci. Int. **173**(1): 1–6. doi:10.1016/j.forsciint.2006.09.013. PMID:17300895.

Dixon, M., and Weiskotten, C. 2016. CITES CoP17: Victory today for pangolins. [Online.] Available from https://newsroom.wcs.org/News-Releases/articleType/ArticleView/articleId/9303/ [accessed 7 October 2005].

Du Toit, Z., Grobler, J.P., Kotzé, A., Jansen, R., Brettschneider, H., and Dalton, D.L. 2014. The complete mitochondrial genome of temminck's ground pangolin (*Smutsia temminckii*; Smuts, 1832) and phylogenetic position of the Pholidota (Weber, 1904). Gene, **551**(1): 49–54. doi:10.1016/j.gene.2014.08.040. PMID:25158133.

Edgar, R.C. 2004. MUSCLE: multiple sequence alignment with high accuracy and high throughput. Nucleic Acids Res. **32**(5): 1792–1797. doi:10.1093/nar/gkh340. PMID:15034147.

Farris, J.S., Källersjö, M., Kluge, A.G., and Bult, C. 1994. Testing significance of incongruence. Cladistics, **10**(3): 315–319. doi:10.1111/j.1096-0031.1994.tb00181.x.

Folmer, O., Black, M., Hoeh, W., Lutz, R., and Vrijenhoek, R. 1994. DNA primers for amplification of mitochondrial cytochrome *c* oxidase subunit I from diverse metazoan invertebrates. Mol. Mar. Biol. Biotechnol. **3**(5): 294–299. doi:10.1371/journal.pone.0013102. PMID:7881515.

Gaubert, P., and Antunes, A. 2015. What's behind these scales? Comments to 'The complete mitochondrial genome of Temminck's ground pangolin (*Smutsia temminckii*; Smuts, 1832) and phylogenetic position of the Pholidota (Weber, 1904)'. Gene, **563**(1): 106–8. doi:10.1016/j.gene.2015.03.021. PMID:25796606.

Gaubert, P., Njiokou, F., Olayemi, A., Pagani, P., Dufour, S., Danquah, E., et al. 2015. Bushmeat genetics: setting up a reference framework for the DNA typing of African forest bushmeat. Mol. Ecol. Resour. **15**(3): 633–651. doi:10.1111/1755-0998.12334. PMID:25264212.

Gaudin, T.J., Emry, R.J., and Wible, J.R. 2009. The phylogeny of living and extinct pangolins (mammalia, pholidota) and associated taxa: a morphology based analysis. J. Mamm. Evol. **16**(4): 235–305. doi:10.1007/s10914-009-9119-9.

Guindon, S., and Gascuel, O. 2003. A simple, fast, and accurate algorithm to estimate large phylogenies by maximum likelihood. Syst. Biol. **52**(5): 696–704. doi:10.1080/10635150390235520. PMID:14530136.

Hasegawa, M., Kishino, H., and Yano, T. 1985. Dating of the human–ape splitting by a molecular clock of mitochondrial DNA. J. Mol. Evol. **21**: 160–174. doi:10.1007/BF02101694.

Hassanin, A., Hugot, J.-P., and van Vuuren, B.J. 2015. Comparison of mitochondrial genome sequences of pangolins (Mammalia, Pholidota). C. R. Biol. **338**(4): 260–265. doi:10.1016/j.crvi.2015.02.003. PMID:25746396.

Hebert, P.D.N., Cywinska, A., Ball, S.L., and deWaard, J.R. 2003. Biological identifications through DNA barcodes. Proc. Biol. Sci. **270**(1512): 313–321. doi:10.1098/rspb.2002.2218. PMID:12614582.

Hsieh, H.M., Chiang, H.L., Tsai, L.C., Lai, S.Y., Huang, N.E., Linacre, A., and Lee, J.C.I. 2001. Cytochrome *b* gene for species identification of the conservation animals. Forensic Sci. Int. **122**(1): 7–18. doi:10.1016/S0379-0738(01)00403-0. PMID:11587860.

Hsieh, H.M., Lee, J.C.I., Wu, J.H., Chen, C.A., Chen, Y.J., Wang, G.B., et al. 2011. Establishing the pangolin mitochondrial D-loop sequences from the confiscated scales. Forensic Sci. Int. Genet. **5**(4): 303–307. doi:10.1016/j.fsigen.2010.06.003. PMID:20638354.

IUCN. 2015. The IUCN red list of threatened species. Version 2015-4. Available from www.iucnredlist.org [accessed 20 January 2016].

Kocher, T.D., Thomas, W.K., Meyer, A., Edwards, S.V., Pääbo, S., Villablanca, F.X., and Wilson, A.C. 1989. Dynamics of mitochondrial DNA evolution in animals: amplification and sequencing with conserved primers. Proc. Natl. Acad. Sci. U.S.A. **86**(16): 6196–6200. doi:10.1073/pnas.86.16.6196. PMID:2762322.

Lagrada, L., Schoppe, S., and Challander, D. 2014. *Manis culionensis*. IUCN Red List Threat. Species 2014: e.T136497A45223365.en. doi:10.2305/IUCN.UK.2014-2.RLTS.T136497A45223365.en.

Masters, B.C., Fan, V., and Ross, H.A. 2011. Species delimitation — a Geneious plugin for the exploration of species boundaries. Mol. Ecol. Resour. **11**(1): 154–157. doi:10.1111/j.1755-0998.2010.02896.x. PMID:21429114.

Mwale, M., Dalton, D.L., Roelofse, M., Radebe, T., Labuschagne, K., Kloppers, A., et al. 2015. Progress in the barcoding of illegally traded South African wildlife species at the National Zoological Gardens of South Africa. Genome, **58**(5): 259–260. doi:10.1139/gen-2015-0087.

Newton, P., Van Thai, N., Roberton, S., and Bell, D. 2008. Pangolins in peril: Using local hunters' knowledge to conserve elusive species in Vietnam. Endanger. Species Res. **6**(1): 41–53. doi:10.3354/esr00127.

Nijman, V., Zhang, M.X., and Shepherd, C.R. 2016. Pangolin trade in the Mong La wildlife market and the role of Myanmar in the smuggling of pangolins into China. Glob. Ecol. Conserv. **5**: 118–126. doi:10.1016/j.gecco.2015.12.003.

Ogden, R., and Linacre, A. 2015. Wildlife forensic science: A review of genetic geographic origin assignment. Forensic Sci. Int. Genet. **18**: 152–159. doi:10.1016/j.fsigen.2015.02.008. PMID:25795277.

Pietersen, D.W., McKechnie, A.E., and Jansen, R. 2014*a*. Home range, habitat selection and activity patterns of an arid-zone population of Temminck's ground pangolins, *Smutsia temminckii*. Afr. Zool. **49**(2): 265–276. doi:10.3377/004.049.0215.

Pietersen, D.W., Waterman, C., Hywood, L., Rankin, P., and Soewu, D. 2014*b*. *Smutsia temminckii*. IUCN Red List Threat. Species: e.T12765A45222717. doi:10.2305/IUCN.UK.2014-2.RLTS.T12765A45222717.en.

Puillandre, N., Lambert, A., Brouillet, S., and Achaz, G. 2012. ABGD, Automatic Barcode Gap Discovery for primary species delimitation. Mol. Ecol. **21**(8): 1864–1877. doi:10.1111/j.1365-294X.2011.05239.x. PMID:21883587.

Qin, X.-M., Dou, S.-R., Guan, Q.-X., Qin, P.-S., and She, Y. 2012. Complete mitochondrial genome of the *Manis pentadactyla* (Pholidota, Manidae): comparison of *M. pentadactyla* and *M. tetradactyla*. Mitochond. DNA, **23**(1): 37–38. doi:10.3109/19401736.2011.643881.

Ratnasingham, S., and Hebert, P.D.N. 2007. BOLD: The Barcode of Life Data System (http://www.barcodinglife.org). Mol. Ecol. Notes, **7**(3): 355–364. doi:10.1111/j.1471-8286.2007.01678.x. PMID:18784790.

Rodrigo, A., Bertels, F., Heled, J., Noder, R., Shearman, H., and Tsai, P. 2008. The perils of plenty: what are we going to do with all these genes? Philos. Trans. R. Soc. B Biol. Sci. **363**(1512): 3893–3902. doi:10.1098/rstb.2008.0173.

Ronquist, F., Teslenko, M., van der Mark, P., Ayres, D.L., Darling, A., Höhna, S., et al. 2012. MrBayes 3.2: Efficient Bayesian phylogenetic inference and model choice across a large model space. Syst. Biol. **61**(3): 539–542. doi:10.1093/sysbio/sys029. PMID:22357727.

Swofford, D.L. 2002. PAUP*. Phylogenetic Analysis Using Parsimony (*and Other Methods). Sinauer Associates, Inc., Sunderland, Mass.

Verma, S.K., and Singh, L. 2002. Novel universal primers establish identity of an enormous number of animal species for forensic application. Mol. Ecol. Notes, **3**(1): 28–31. doi:10.1046/j.1471-8286.2003.00340.x.

Waterman, C., Pietersen, D., Hywood, L., Rankin, P., and Soewu, D. 2014*a*. *Smutsia gigantea*. IUCN Red List Threat. Species 2014: e.T12762A45222061. doi:10.2305/IUCN.UK.2014-2.RLTS.T12762A45222061.en.

Waterman, C., Pietersen, D., Soewu, D., Hywood, L., and Rankin, P. 2014*b*. *Phataginus tetradactyla*. IUCN Red List Threat. Species 2014: e.T12766A45222929.en. doi:10.2305/IUCN.UK.2014-2.RLTS.T12766A45222929.en.

Waterman, C., Pietersen, D., Soewu, D., Hywood, L., and Rankin, P. 2014*c*. *Phataginus tricuspis*. IUCN Red List Threat. Species: e.T12767A45223135. doi:10.2305/IUCN.UK.2014-2.RLTS.T12767A45223135.en.

Zhang, H., Miller, M.P., Yang, F., Chan, H.K., Gaubert, P., Ades, G., and Fischer, G.A. 2015. Molecular tracing of confiscated pangolin scales for conservation and illegal trade monitoring in Southeast Asia. Glob. Ecol. Conserv. **4**: 414–422. doi:10.1016/j.gecco.2015.08.002.